

# Polyelectrolyte Substrate Coating for Controlling Biofilm Growth at Solid–Air Interface

Nikolay V. Ryzhkov, Anna A. Nikitina, Peter Fratzl, Cécile M. Bidan,\*  
and Ekaterina V. Skorb\*

Because bacteria–surface interactions play a decisive role in bacteria adhesion and biofilm spreading, it is essential to understand how biofilms respond to surface properties to develop effective strategies to combat them. Polyelectrolyte coating is a simple and efficient way of controlling surface charge and energy. Using polyelectrolytes of various types, with different molecular weights and polyelectrolyte solutions of various pH provides a unique approach to investigate the interactions between biofilms and their substrate. Here, the formation of *Escherichia coli* biofilms at a solid–air interface is explored, whereby charge and interfacial energy are tuned using polyelectrolyte coatings on the surface. Cationic coatings are observed to limit biofilm spreading, which remain more confined when using high molecular weight polycations. Interestingly, biofilm surface densities are higher on polycationic surfaces despite their well-studied bactericidal properties. Furthermore, the degree of polyelectrolyte protonation also appears to have an influence on biofilm spreading on polycation-coated substrates. Finally, altering the interplay between biomass production and surface forces with polyelectrolyte coatings is shown to affect biofilm 3D architecture. Thereby, it is demonstrated that biofilm growth and spreading on a hydrogel substrate can be tuned from confined to expanded, simply by coating the surface using available polyelectrolytes.

consequences on human health<sup>[1,2]</sup> and industrial processes<sup>[3,4]</sup> as well as antibiotics resistance.<sup>[5]</sup> Various approaches to inhibition of biofilm formation and their eradication were developed.<sup>[6]</sup> Biofilm formation at an interface is determined by several phenomena, e.g., the initial adhesion of single bacteria to the surface and the further biofilm growth and spreading due to cell proliferation and biopolymer production.<sup>[7]</sup> Therefore, surface energy and electrostatic interactions with the substrate are two key determinants of biofilm formation. On this basis, a common strategy to fight bacterial colonization is the functionalization of surfaces that are prone to biofilm fouling.<sup>[6,8]</sup> For instance, surface hydrophilization<sup>[9]</sup> and low surface energy strategies<sup>[10]</sup> were considered. Surface topology was also modified to influence bacterial colonization, as recently reviewed in detail.<sup>[11]</sup>

Polyelectrolyte coatings allow changing the surface energy, charge, and mechanical characteristics of various substrates easily.<sup>[12,13]</sup> Therefore, polyelectrolyte assemblies are often considered for possible application as antibacterial coatings. However, understanding the fundamental principles of bacteria–surface interactions remains of high importance.<sup>[14–16]</sup> Due to the negative charges found on their external membrane, bacteria tend to tightly attach to positively charged surfaces.<sup>[17]</sup> It was demonstrated that biofilm spreading rate was decreasing with increasing strength of adhesion.<sup>[17]</sup> One possible explanation is that bacteria elongation preceding cell division is obstructed by strong electrostatic binding to the surface.<sup>[18]</sup> Besides this, it is also known that positively charged molecules (and polycations to a greater extent) exhibit antibacterial properties due to their ability to disrupt membranes of bacterial cells.<sup>[19]</sup> In contrast, negatively charged surfaces provide less stable bacterial cell contact with the surface,<sup>[18]</sup> so that the initial adhesion step is difficult but further biofilm spreading meets less obstacle.


In addition to help preventing healthcare and industry-related issues, investigating biofilm formation is beneficial to understand the development of biological tissues,<sup>[20]</sup> cell adaptability,<sup>[21]</sup> and communication<sup>[22]</sup> since some morphogenesis principles are common with higher organisms' tissues. Furthermore, colonies and biofilms of non-pathogenic microorganisms are considered to be promising to design hybrid living materials<sup>[23–27]</sup> challenging to get synthetically. Revealing

## 1. Introduction

Biofilms are surface-attached complex 3D structures of bacterial cells embedded in a self-produced fibrous biopolymer matrix. These adhesive living systems are known for their

N. V. Ryzhkov, A. A. Nikitina, Prof. E. V. Skorb  
Infochemistry Scientific Center of ITMO University  
ITMO University  
Lomonosova str. 9, St. Petersburg 191002, Russia  
E-mail: skorb@itmo.ru

Prof. P. Fratzl, Dr. C. M. Bidan  
Biomaterials Department  
Max Planck Institute of Colloids and Interfaces  
Am Mühlenberg 1, 14424 Potsdam, Germany  
E-mail: cecile.bidan@mpikg.mpg.de

 The ORCID identification number(s) for the author(s) of this article can be found under <https://doi.org/10.1002/admi.202001807>.

© 2021 The Authors. Advanced Materials Interfaces published by Wiley-VCH GmbH. This is an open access article under the terms of the Creative Commons Attribution-NonCommercial-NoDerivs License, which permits use and distribution in any medium, provided the original work is properly cited, the use is non-commercial and no modifications or adaptations are made.

DOI: 10.1002/admi.202001807

the nature of bacteria–surface interactions and identifying the principles of biofilm adaptation to surface conditions are also essential to support further progresses in such contexts.

Polyelectrolytes are charged polymers that are able to change their characteristics in response to external stimuli such as temperature,<sup>[28]</sup> light,<sup>[29]</sup> ionic strength,<sup>[30]</sup> and pH.<sup>[31,32]</sup> It was recently demonstrated that reversible oscillation of polyelectrolyte layer-by-layer assemblies based on high amplitude actuation of block copolymer micelles allows controlling cell behavior on a surface. Their pH responsiveness was also used via light–pH coupling<sup>[33]</sup> to control the behavior of mammalian cells.<sup>[34,35]</sup>

Here, we chose an *Escherichia coli* strain (*E. coli* AR3110)<sup>[36]</sup> to study biofilm formation on polyelectrolyte-modified agar gels. *E. coli* AR3110 bacteria were shown to produce and assemble an extracellular matrix mainly composed of phosphoethanolamine cellulose and amyloid fibers.<sup>[36,37]</sup> We found that the patterns of ridges and wrinkles emerging during biofilm growth on solid depend on the nature of the polyelectrolyte used, its molecular weight, and the pH of the solution in which it was prepared. Macroscopic spatiotemporal characterizations of the biofilms were performed to assess the influence of the physicochemical properties of the substrates on biofilms morphology. We believe that the phenomena discovered in our study can make a significant contribution to understanding the adaptability of biological tissues and be used in the development of approaches to the directed biosynthesis of functional materials. In addition, the data shown will help to develop more effective ways to prevent biofilm growth in both medical and industrial contexts.

## 2. Results and Discussion

We used various polyelectrolytes to modify the surface properties of the nutritive substrate in order to control *E. coli* AR3110 biofilm growth. Therefore, we chose several polyelectrolytes,

namely polyethyleneimine (PEI; weak polycation), poly(sodium 4-styrenesulphonate) (PSS; strong polyanion), poly(allylamine hydrochloride) (PAH; weak polycation), and poly(acrylic acid) (PAA; weak polyanion) (Figure S1, Supporting Information). We varied the conditions of polyelectrolyte deposition by using different molecular weights of the polycations. The molecular weight allows affecting the transformation from glassy and rubbery states of the polyelectrolyte.<sup>[38]</sup> Various pH in the polyelectrolyte solutions were used for their deposition.

### 2.1. Polycationic Surfaces Impair Biofilm Spreading and Limit Their Growth

Polyelectrolyte solutions used for coating deposition were adjusted to pH 7. Detailed insight of biofilm morphogenesis on the various polyelectrolyte coatings were obtained by capturing images every 30 min and gathering them in time-lapse videos (see Videos, Supporting Information). Figure 1a demonstrates the appearance of biofilms growing on bare and polyelectrolyte coated agar substrates at various time points. Differences in the speed of biofilm spreading and, in their phenotype, depending on the polyelectrolyte used could be observed. Daily measurements of projected biofilm area were plotted as a function of time (Figure 1b).

Figure 1a,b shows that biofilm growth kinetics was similar on a bare Luria-Bertani (LB) agar and on PSS- or PAA-coated LB agar throughout the entire observation time. They demonstrate synchronous growth and the same projected area throughout the observation period as well as the same final mass after 4 days of growth. In contrast, cationic polymers were observed to significantly reduce biofilm spreading over the substrate. In particular, *E. coli* biofilms grown on PEI ( $M_w = 25\,000$ ) or PAH ( $M_w = 17\,000$ ) covered agar substrate after 4 days of incubation had on average a diameter  $\approx 2.5$  times smaller than control biofilms grown on bare agar substrates.

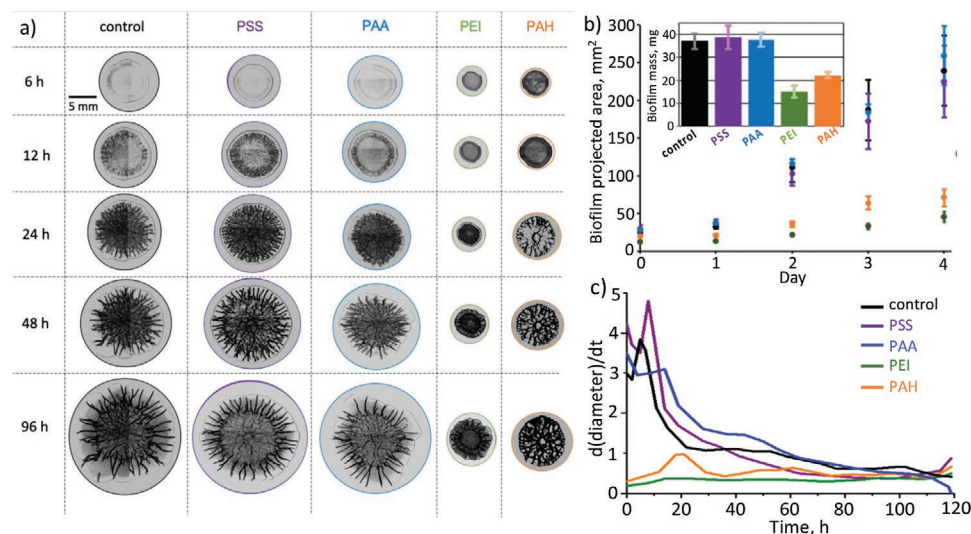


**Figure 1.** a) Bright-field snapshots of biofilms growing on bare control and polyelectrolyte-covered (PSS, PAA, PEI ( $M_w$  25 000), PAH ( $M_w$  17 000)) agar substrates at designated times. b) Biofilm projected area plotted versus incubation time and biofilm mass data (inset): biofilms grown on PAA, PSS coatings, and control surface demonstrate the same values of the projected area ( $p > 0.1$ ) and mass ( $p = 0.8$ ), whereas PEI and PAH coatings promote smaller biofilm area ( $p < 0.002$ ) throughout the observation period and final mass ( $p < 2 \times 10^{-5}$ ), herewith PEI reduces biofilm spreading more than PAH ( $p < 0.003$  for area and  $p = 8 \times 10^{-4}$  for mass). c) Derivative plot of biofilm versus time of growth.

After inoculation, biofilm growth rate on the control as well as on polyanion-coated surfaces (PAA and PSS) were higher than on polycation-coated surfaces (PEI and PAH). The biofilm projected area of biofilm growing on a pristine agar surface (as well as on PSS and PAA coated) increase by about 30% on the first day, and 300% on the second day with a subsequent slowdown (Figure 1b). But for biofilms growing on PEI- and PAH-coated agar, significantly slower growth rate was observed. On the first day, biofilms grew by only 8% and 12%, respectively, whereas on the second day by 57% (PEI) and 70% (PAH) (Figure 1b). After 4 days of culture, biofilms grown on polycationic surfaces occupied less than 20% of control biofilm area (Figure 1b inset). Kymograph-like space–time plots showing changes of biofilm diameter as a function of time were extracted from time-lapse videos (Figure S2a, Supporting Information). The temporal evolution of biofilm diameter was additionally plotted for each type of polyelectrolyte coating (Figure S2b, Supporting Information).

Derivative plots were also obtained to better visualize and quantify the growth rate (Figure 1c). Biofilms growing on positively charged surfaces (PEI- and PAH-coated agar) were characterized by a slow growth at an almost constant rate (with a small maximum for PEI). Biofilms growing on negatively charged surfaces first grow faster reaching a maximum growth rate between 5 and 7 h after inoculation, and subsequently slowed down to reach similar growth rates as those observed on positively charged surfaces (less pronounced for PAA in this experiment) (Figure 1c).

After 4 days of growth, biofilms were removed from the nutritive substrates and weighted. The average mass of biofilms grown on surfaces covered by various polyelectrolytes is displayed in the insert in Figure 1b. The biofilms grown on PEI and PAH were 2 to 2.5 times lighter than the ones grown on the control surfaces, although their area was more than five times lower (Figure 1b). In other words, biofilm growing on polycation-coated substrates was two times denser than biofilm growing on bare control or PSS- and PAA-covered surfaces (32–33 vs 14–19 mg cm<sup>-2</sup>) (Figure S3a, Supporting Information). Interestingly, PEI and PAH constrained biofilm spatial expansion but did not impair biomass production to the same degree.

It has been reported that polycations exhibit antibacterial properties, i.e., interact with and disrupt bacterial cell membranes.<sup>[39,40]</sup> But PEI and PAH coatings were reported to exhibit weak bactericidal activity since they do not contain the quaternary amino groups most toxic to bacteria.<sup>[14,41]</sup> Indeed, biofilms inoculated from bacterial suspension in nutritive media mixed with polycation solution revealed no bactericide effect of polycation. It was evidenced by the fact that biofilms grew equally regardless of the nature of the polyelectrolyte when a bare agar plate was inoculated with bacterial suspension mixed with these polyelectrolyte solutions (Figure S4, Supporting Information). Hence, the reason for limited biofilm spreading on polycationic surfaces rather lies in interfacial effects than in polyelectrolyte toxicity. We assume that biofilm spreading is impaired by strong electrostatic attachments, which prevent elongation and division of the bacteria along the plane of the solid-air interface.<sup>[17,42]</sup> A so-called “arrested growth”<sup>[43]</sup> behavior was consistently observed for biofilms forming on PEI- and PAH-coated substrates. Concerning surface energy, it was reported that surface charging usually improves wetting

properties<sup>[44]</sup> without clear correlation between the sign of charge and wettability.<sup>[12]</sup> However, some studies report that polyelectrolyte multilayers with terminating polycations tend to be more hydrophobic,<sup>[45]</sup> which also may have an impact in our case. Our observations are expected to hold for both negatively charged gram-positive and gram-negative bacteria, which were shown to both adhere faster on positively charged surfaces compared to negatively charged ones. However, the effects may be slightly altered in gram-positive bacteria, which were shown to better grow on positive surfaces compared to gram-negative bacteria in dynamic conditions.<sup>[18]</sup> However, it should be noted that the shape of the bacterial cell may also play a role in the process under investigation, so it is difficult to make unambiguous assumption about how polyelectrolyte coatings affect the growth of biofilms of bacteria with different cell membrane structures without taking into account many other factors. Therefore, in this study, we focused on studying the effects on a single bacteria type: *E. coli* AR 3110.

## 2.2. High-Molecular-Weight Coatings Suppress Biofilm Spreading

Since polyanionic coatings did not significantly affect biofilm morphogenesis, we further focused on polycations. PEI of several molar weights was used to coat the surface of the nutritive LB agar biofilm substrates. Biofilm images were acquired daily during the culture period and the projected biofilm area was measured and plotted against time (Figure 2). The increase of molar weight of the polycations resulted in a decreasing speed of biofilm spreading.

In comparison to bare substrates (control), biofilms reached 50–60% of the control projected area when grown on low molecular weight ( $M_w = 1300$ ) PEI-coated substrates, 20–30% on medium molecular weight ( $M_w = 25\ 000$ ) PEI-coated substrates, and only ≈10% on high molecular weight ( $M_w = 750\ 000$ ) PEI-coated substrates (Figure 2a).

The ratio of the mass of biofilms grown on PEI coated substrate to the control conditions was 0.7, 0.4, and 0.25 for low, medium, and high molecular weight PEI, respectively, (Figure 2a inset). Area density, in contrast, increased from 23 to 35 mg cm<sup>-2</sup> upon transition from the surface modified by low weight PEI to high weight PEI (Figure S3b, Supporting Information).

Similar to PEI, increasing PAH molecular weight in PAH-coated LB agar substrates from 17 000 to 65 000 led to a decrease of the projected area and the mass of the biofilms grown on their surface (Figure 2b and inset) and an increase of the area density (30 mg cm<sup>-2</sup> for low molecular weight vs 40 mg cm<sup>-2</sup> for high molecular weight polymer) (Figure S3c, Supporting Information).

This is consistent with the data on the dependence of the hydrophobicity of polyelectrolyte coatings on their molecular weight. For alkylated PEI derivatives antibacterial activity was revealed to depend on the molecular weight of the polymer.<sup>[14]</sup> Low molecular weight polymers were reported to have negligible, if any, antibacterial activity.<sup>[14]</sup> Indeed, for PEI and PAH, each repeat unit of both polycations carries two hydrophobic CH groups together with protonatable and potentially hydrophilic NH groups. Hence, polymer molecular weight increase promotes worse wettability.

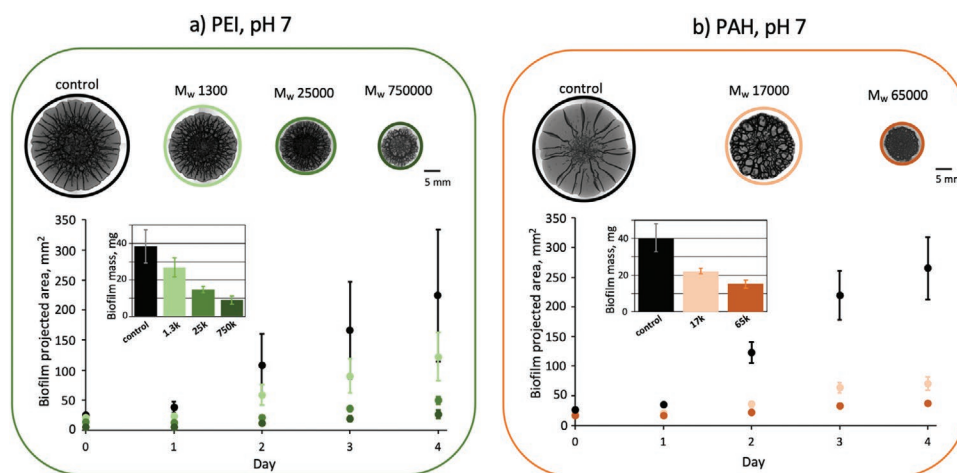


**Figure 2.** Effect of polyelectrolyte molecular weight: a) bright-field images (top) of biofilms grown for 4 days on bare nutritive agar substrate and substrate covered by PEI with average  $M_w = 1300$ , average  $M_w = 25\,000$ , and average  $M_w = 750\,000$ ; biofilm projected area versus incubation time (bottom), inset demonstrates biofilm mass data after 4 days of growth; the area and mass of a biofilm grown on PEI coating with medium molecular weight is less than on low molecular weight ( $p < 3 \times 10^{-4}$  and  $p < 2 \times 10^{-5}$ , respectively) and more than on high molecular weight coating ( $p < 7 \times 10^{-7}$  and  $p < 5 \times 10^{-5}$ , respectively). b) Bright-field images (top) of biofilms grown for 4 days on bare nutritive agar substrate and substrate covered by PAH with average  $M_w = 17\,000$ , average  $M_w = 65\,000$ ; biofilm projected area versus incubation time (bottom), inset demonstrates biofilm mass data after 4 days of growth; the area and mass of a biofilm grown on high molecular weight PAH coating is less than on low molecular weight coating ( $p < 2 \times 10^{-7}$  and  $p < 0.002$ , respectively).

### 2.3. The pH of the Polyelectrolyte Solutions Used to Coat the Agar Has a Conditional and Limited Effect on Biofilm Spreading

Branched PEI is known for its buffering capacity. It is a weak polycation highly sensitive to pH of surrounding media and responding to it by charge and conformational alterations.<sup>[46,47]</sup> We deposited PEI ( $M_w = 25\,000$ ) from solutions of various pH (Figure 3a). This molecular weight was chosen for giving

a clear effect on biofilm morphology, while leaving the possibility to observe further limitation of biofilm spreading. Indeed, with the more effective  $M_w = 750\,000$ , further biofilm growth limitation induced by pH changes would be difficult to quantify due to their size similar to the initial drop of bacteria suspension. At all studied pH (3, 5, 7, and 9), biofilm growth was much reduced compared with the control experiment on bare agar substrate, for which the pH of the aqueous phase in

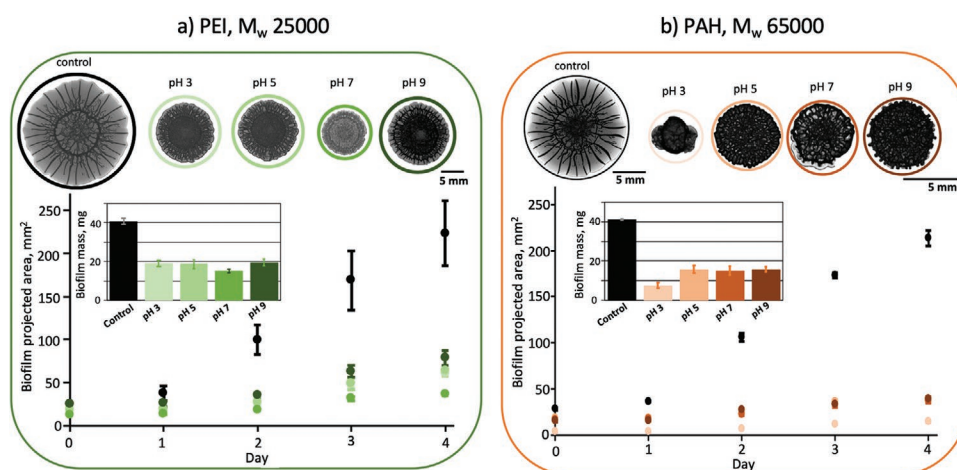


**Figure 3.** Effect of the pH of the polyelectrolyte solutions: a) bright-field images (top) of biofilms grown for 4 days on bare nutritive agar substrate and substrate covered by PEI with average  $M_w = 25\,000$  and pH 3, 5, 7, and 9; biofilm area versus incubation time (bottom); and biofilm mass data after 4 days of incubation (inset); PEI coating applied from solution with pH 7 limits biofilm spreading as well as mass production to the greatest degree ( $p < 6 \times 10^{-4}$  and  $p = 1 \times 10^{-5}$ , respectively), whereas areas and masses of biofilms grown at PEI coating applied from solutions with pH 3, 5, and 9 are equal ( $p > 0.01$  and  $p > 0.06$ , respectively). b) Bright-field images (top) of biofilms grown for 4 days on bare nutritive agar substrate and substrate covered by PAH with average  $M_w = 65\,000$  and pH 3, 5, 7, and 9; biofilm area versus incubation time (bottom); and biofilm mass data after 4 days of incubation (inset); PAH coating applied from solution with pH 3 limits biofilm spreading as well as mass production to the greatest degree ( $p < 3 \times 10^{-6}$  and  $p = 0.001$ , respectively), whereas areas and masses of biofilms grown at PAH coatings applied from solutions with pH 5, 7, and 9 are equal ( $p > 0.06$  and  $p > 0.8$ , respectively).

the hydrogel was estimated between 7 and 8 using pH paper. Surprisingly, the effect was particularly pronounced on the substrate coated with a neutral PEI solution of pH 7. In this case, the projected area of the biofilms on the fourth day was 2 to 2.5 times smaller and their mass was  $\approx 20\%$  lower compared to the biofilms obtained with all the other tested pH. Moreover, the area density of biofilms grown on PEI coatings was maximum at pH 7 (34 vs 25–30 mg cm<sup>-2</sup> for other studied pH) (Figure S3d, Supporting Information). Here, we can also note that depositing a drop of basic or acidic solution (without polyelectrolyte) on the agar surface prior to inoculation did not affect further biofilm growth and spreading (Figure S5, Supporting Information).

We believe that the observed phenomenon can be explained by the non-monotonicity of changes in the properties of PEI as a function of pH. A freshly prepared solution of PEI in 0.5 M NaCl has a pH 9. The polymer charge increases with decreasing pH. Due to PEI protonation, the surface coated at pH 7 carries a more positive net charge in comparison to the surface coated at pH 9, and thus is more favorable to the adhesion of negatively charged bacteria. As a result, biofilm spreading on the surface coated at pH 7 is limited to a greater extent. With further protonation, the protonability of amine groups decreases due to electrostatic repulsion of protons from already protonated amine groups.<sup>[48]</sup> As a result, more protons and chloride ions are found in solution as HCl is added to reach lower pH values. Eventually, chloride ions screen the positive charges of protonated amines, which leads to a decrease of the positive net charge. Therefore, agar substrates coated with PEI at pH 3 and 5 are expected to present lower positive net charges compared to pH 7 and thereby weaker electrostatic interactions with bacteria. Consistently, a better spreading of biofilm over these surfaces coated at pH 3 and 5 was observed in comparison to pH 7.

PAH is another weak polyelectrolyte with a pKa from 8.5 to 9 and has buffering capacity.<sup>[49,50]</sup> Low molecular weight PAH ( $M_w = 17\,000$ ) demonstrated ambiguous data on pH-dependence (Figure S6, Supporting Information). However, for high molecular weight PAH ( $M_w = 65\,000$ ), biofilm spreading was impaired to the greatest degree on a surface coated with a PAH solution of pH 3. On such an acidic surface, the biofilm spread over approximately one-third of the projected area and weighted approximately half of the mass compared to biofilms growing on surfaces modified with PAH from solutions with less acidic pH (from 5 to 9) (Figure 3b). On PAH coatings, the largest value of biofilm area density was obtained at pH 3 (54 mg cm<sup>-2</sup> vs 40 for pH 5–9) (Figure S3e, Supporting Information). Thus, we found that the polycations that inhibit the spreading of biofilms also presented a pH-dependent effect on biofilm growth.

Decreasing the pH of PAH solution gradually increases the degree of PAH molecule protonation. Unlike branched PEI, protonated amino groups of the PAH are not located in the backbone and are thus more accessible to protonation. Therefore, protonation is accompanied by a monotonous increase of polymer molecule positive charge and gradual conformational transition from coiled to extended. As a result, the hydrophobicity and the charge of surfaces coated by PAH increase as the pH decreases.

Polyanions did not exhibit such an effect and biofilms grown on surfaces modified with PAA and PSS were similar

to control samples. To reveal pH dependence of polyanion coatings, solutions of weak polyanion–polyacrylic acid (PAA, pKa = 4.5–6.5<sup>[51,52]</sup>) with various pH were prepared and used to coat agar substrates where biofilms were grown. When the carboxyl groups are protonated, the polymer is overall hydrophobic. On the other hand, when deprotonated, the surface is expected to be less hydrophobic. Hence, PAA-coated agar is expected to be more hydrophobic in comparison with a less protonated and more negatively charged PAA surface at higher pH. In contrast to this assumption, we did not observe any influence of PAA coating pH on biofilm spreading (Figure S7, Supporting Information). Apparently, the charge effect prevails over the wettability of the surface on which the biofilm grows. As long as the surface charge remains negative, the biofilm hydrophobicity does not constitute a major obstacle to biofilm growth.

#### 2.4. Polyelectrolyte Coating Affects Biofilm Wrinkling Patterns

Mechanical and adhesive properties of the biofilms were shown to determine their morphology.<sup>[53]</sup> The different biofilm sizes and shapes obtained on the different types of polyelectrolyte coatings may thus provide insights into the biofilm properties involved in the effects observed and thereby provide new hints on how to control them. After inoculation of bare agar substrates, *E. coli* AR3110 expanded and formed circular biofilms with disordered wrinkling patterns in the center and radial folds on the outside. Biofilms grown on PSS or PAA coated substrates were also characterized by more disorganized patterns in the core and radial wrinkles emerging at the periphery (Figure 4a,b). In contrast, biofilms grown on PEI- and PAH-coated substrates developed a more compact morphology characterized by very dense networks of poorly organized wrinkles (Figure 4a,c). It was reported that periodical radial wrinkles developing in biofilms originate from tangential compressive stresses that accumulate during growth and cannot be released otherwise, while radial stresses are released by biofilm expansion.<sup>[53]</sup> These conclusions are in line with our observation that the wrinkling patterns obtained on various surfaces vary from periodic radial folds with low density (on bare substrates, PSS and PAA) to very dense and disordered folding patterns (on PEI and PAH). This qualitative observation is supported by the calculation of the biofilm area density (biofilm mass/biofilm projected area), which appears to vary accordingly from  $\approx 20$  mg cm<sup>-2</sup> in control conditions or on polyanionic surfaces to values greater than 40 mg cm<sup>-2</sup> on polycationic surfaces (Figure S8, Supporting Information, inset). It highlights that despite a lower mass, biofilms subjected to constrained spreading on polycationic coatings have a higher area density compared to control surfaces and polyanionic coatings. This observation indicates that the interfacial interactions with the substrate affect the biofilm lateral spreading in a greater extent than biomass production. The mechanism of radial stress relaxation through biofilm expansion along the surface<sup>[53]</sup> is thus less effective in cases of confined spreading like on polycationic surfaces, so that compressive stresses are expected to build up in both radial and circumferential directions and lead to the observed disordered and dense wrinkling pattern (Figure 4a,c).

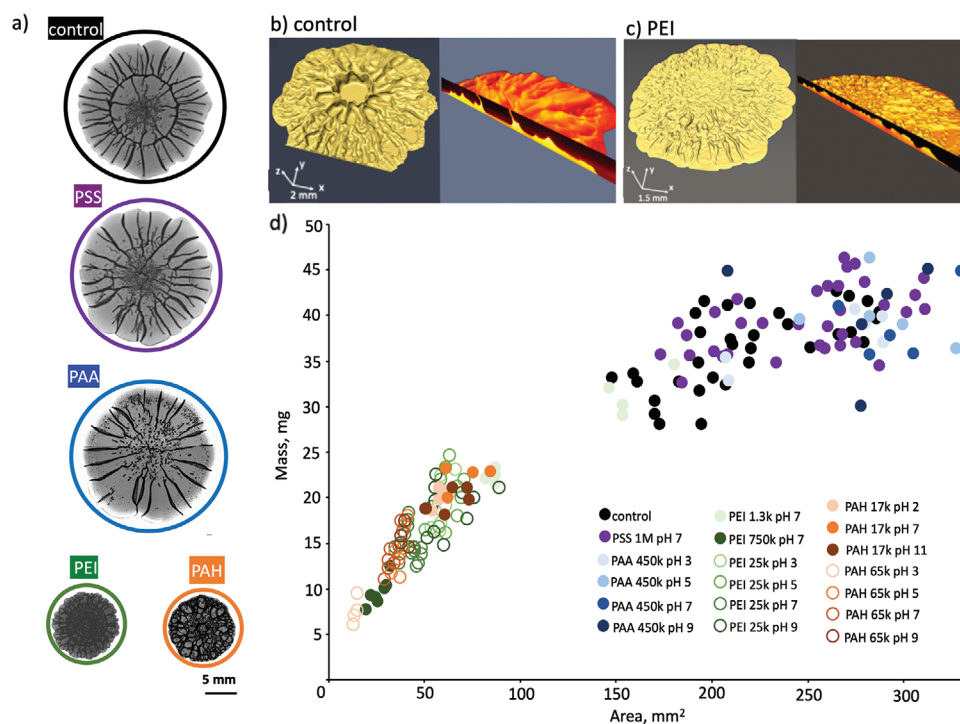


**Figure 4.** a) Bright-field images of biofilms grown for 4 days on a bare nutritive agar substrate PSS-, PAA-, PEI-, and PAH-coated substrates; b,c) X-ray microtomographies of biofilms grown on b) a bare agar substrate and c) a PEI-coated agar substrate; d) scatter diagram of mass and area for biofilms growing on substrates coated by various polyelectrolytes of different molecular weight and pH.

To better understand the link between biofilm morphology and the properties of the underlying surface, we plotted each biofilm mass as a function of their projected area for all the conditions tested (Figure 4d). Two data clusters are clearly separated by a gap at areas between 100 and 150 mm<sup>2</sup>: one corresponds to biofilm confined spreading on polycationic coatings and the other corresponds to biofilm expanded spreading on bare agar substrates or polyanionic coatings. Biofilms grown on PEI coatings with  $M_w$  25 000 and pH 3, 5, and 9 were found to have no statistically significant differences in area and mass ( $p > 0.01$ ) and, therefore, were combined into one group. Similarly, we combined the data for biofilms grown on PAH coatings with  $M_w$  17 000 and separately for biofilms grown on PAH with  $M_w$  65 000 and pH 5, 7, and 9. Data for PSS, PAA, and control were also combined following the same criterion. In Figure S8 (Supporting Information) one can see that the data are divided into a larger number of clusters with varying degrees of positive correlation within each of them. Figure S8 (Supporting Information) shows that the clusters corresponding to biofilms grown on PAH  $M_w$  65 000 (pH 5, 7, and 9) and PEI  $M_w$  25 000 (pH 7) overlap significantly and have similar values of density but different phenotypes: disordered wrinkled cores and radial wrinkled shells on PEI and completely disordered wrinkling on PAH (Figure 3). Similarly, clusters formed by biofilms of different phenotypes grown on PAH  $M_w$  17 000 and PEI  $M_w$  25 000 (pH 3, 5, and 9) also intersect. Thus, the effect of polyelectrolyte coatings on biofilm 3D architecture is not limited to creating obstacles to lateral spreading on the surfaces but has a more complex nature, which is still unclear. In that context, it will be worthwhile to

explore further how the polyelectrolyte coating affect biofilm composition and if polyelectrolytes from the coating interact with biofilm matrix components. The simple experimental protocol for systematic studies of the effect of polyelectrolyte coatings on biofilm growth established in this work will be the ideal tool to address this new question with various bacteria types, shapes, and matrices, in a near future.

### 3. Conclusion

*E. coli* AR3110 biofilms were grown on polyelectrolyte-coated agar substrates. Polyelectrolyte coating is a convenient approach to modify surface charge and energy to influence biofilm formation at solid–air interfaces in static conditions. It was demonstrated that polycationic surfaces impair biofilm spreading on their substrate. It was also surprisingly observed that polycation coatings, which are considered to be antibacterial, lead to the formation of denser biofilms. Increasing the molecular weight of the polycations used to coat the substrate impairs biofilm spreading even more. For weak polyelectrolyte coatings, pH dependence of biofilm spreading over such coatings revealed that more protonated surfaces prevent biofilm spreading to larger extent thus confirming the role of charges. In addition, it was shown that polyelectrolyte coating influences both the area of spreading and (to a smaller extent) the amount of produced biomass, thereby influencing the 3D architecture of biofilm growing on a particular substrate. We, thus, demonstrated that biofilm spreading can be confined or extended by modifying the substrate with common polyelectrolytes.

## 4. Experimental Section

**Chemicals:** Branched PEI ( $M_w = 1300$ ,  $M_w = 25\,000$ , and  $M_w = 750\,000$ ), PAH ( $M_w = 17\,000$ ,  $M_w = 65\,000$ ), PSS ( $M_w = 1\,000\,000$ ), and PAA ( $M_w = 450\,000$ ) were purchased from Sigma-Aldrich. LB (Luria/Miller) nutrient media from Roth was used to obtain a bacterial suspension. Microcolonies were grown on LB agar (Luria/Miller) from Roth. The biofilms were grown on 15 cm diameter plates of NaCl-free LB agar containing 10 g L<sup>-1</sup> tryptone from casein, 1.25 g L<sup>-1</sup> yeast extract, and 18 g L<sup>-1</sup> bacteriologic agar (all from Roth).

**Substrate Preparation:** NaCl-free LB agar solutions were prepared from the ingredients listed above and autoclaved. The solutions were then kept warm in a water bath at 55 °C for 1 h before pouring 100 mL per 15 cm petri dish. After solidification of the agar, the plates were sealed with parafilm and kept upside down for 2 days at room temperature. Several 2 mg mL<sup>-1</sup> solutions of polyelectrolytes were prepared in 0.5 M NaCl. The pH of each solution was adjusted to the desired values by dropping NaOH and HCl. Further, polyelectrolyte solutions with adjusted pH were sterilized using filtration and UV irradiation. The surface of each large NaCl-free LB agar plate was virtually divided into nine sections. One of the sections was not coated with polyelectrolytes. Having such a control in each plate enables to account for the interplate variability of biofilm phenotypes caused by parameters not considered in the experiment (e.g., humidity in the laboratory). On each of the eight remaining sections, 50 µL of the corresponding polyelectrolyte solution was deposited with a pipette and allowed to spontaneously spread over the surface. The polyelectrolyte films obtained on the agar surface were finally left to dry for 30–40 min without the lid of the plate.

**Biofilm Culture:** *E. coli* AR3110 bacteria (kindly provided by the Microbiology Lab of the Humboldt University, Berlin, Germany) were used. Bacterial suspension was routinely obtained by growing single microcolonies overnight in liquid LB medium. Each section of the polyelectrolyte coated NaCl-free LB agar plates (including control) were inoculated with 5 µL of bacterial suspension as a single round drop (without bubbles). After the inoculation drop had dried on the surface of the agar, the plates were closed, sealed with parafilm, turned upside down, and incubated at 28 °C for up to 4 days. All these steps were performed under a sterile laminar flow.

**Biofilm Characterization:** Once a day, each inoculated plate was imaged with a regular scanner. The biofilm images were analyzed using ImageJ<sup>[54]</sup> to quantify biofilm growth by measuring the projected biofilm area as a function of culture time. For detailed macroscopic spatiotemporal characterizations of biofilm geometry, a separate series of growth experiments was carried out in a specially designed transparent incubator installed on the stage of a stereomicroscope (Zeiss AxioZoom.V16). Each of the nine biofilms growing on the same plate was imaged separately every 30 min for 4 days. The images of each biofilm were then combined to produce time-lapse videos. Part of the biofilms was scanned with an X-ray microtomography scanner (EasyTom, RX Solutions), provided with a micro-focus tube (XRay150, RX-Solutions). Image stacks were reconstructed in the X-ACT software (RX-Solutions). For visualization, slice conjunction and 3D rendering were performed in Amira (Version 6.5, FEI). After 4 days of growth, each biofilm was removed from the nutritive substrate, placed in a separate tube, and weighted. The obtained mass values were averaged and presented with their standard deviation.

**Statistics:** Between 10 and 15 experiments were carried out in each of the conditions studied. The data are presented as mean values with standard deviations. The null hypothesis regarding the equivalence of data obtained under different experimental conditions was tested using one-way analysis of variance. Differences in experimental data with  $p < 0.01$  were considered to be statistically significant.

## Supporting Information

Supporting Information is available from the Wiley Online Library or from the author.

## Acknowledgements

This work was financially supported by Russian Science Foundation, grant no. 19-19-00508. ITMO Fellowship and Professorship Program are acknowledged for infrastructural support. N.V.R. thanks RFBR for support according to the research project no. 19-33-90163. The authors are grateful to Regine Hengge (HU Berlin) for providing the *E. coli* strain AR3110.

Open access funding enabled and organized by Projekt DEAL.

## Conflict of Interest

The authors declare no conflict of interest.

## Data Availability Statement

The data that support the findings of this study are available from the corresponding author upon reasonable request.

## Keywords

adhesion, biofilms, polyelectrolyte coatings, polymer interfaces, wetting

Received: October 14, 2020

Revised: December 30, 2020

Published online: March 18, 2021

- [1] K.-Y. Ha, Y.-G. Chung, S.-J. Ryoo, *Spine* **2005**, *30*, 38.
- [2] D. Pavithra, M. Doble, *Biomed. Mater.* **2008**, *3*, 034003.
- [3] J. J. Kelly, N. Minalt, A. Culotti, M. Pryor, A. Packman, *PLoS One* **2014**, *9*, e98542.
- [4] D. Kregiel, *Food Control* **2014**, *40*, 32.
- [5] P. S. Stewart, J. W. Costerton, *Lancet* **2001**, *358*, 135.
- [6] D. Huang, J. Wang, K. Ren, J. Ji, *Biomater. Sci.* **2020**, *8*, 4052.
- [7] G. O'toole, H. B. Kaplan, R. Kolter, *Annu. Rev. Microbiol.* **2000**, *54*, 49.
- [8] L. Liu, H. Shi, H. Yu, S. Yan, S. Luan, *Biomater. Sci.* **2020**, *8*, 4095.
- [9] Y. F. Yang, L. S. Wan, Z. K. Xu, *Water Sci. Technol.* **2010**, *61*, 2052.
- [10] J. Lee, J. Yoo, J. Kim, Y. Jang, K. Shin, E. Ha, S. Ryu, B. G. Kim, S. Wooh, K. Char, *ACS Appl. Mater. Interfaces* **2019**, *11*, 6550.
- [11] S. Guo, M. Y. Kwek, Z. Q. Toh, D. Pranantyo, E. T. Kang, X. J. Loh, X. Zhu, D. Jariczewski, K. G. Neoh, *ACS Appl. Mater. Interfaces* **2018**, *10*, 7882.
- [12] K. Hänni-Ciunel, G. H. Findenegg, R. V. Klitzing, *Soft Mater.* **2007**, *5*, 61.
- [13] N. V. Ryzhkov, D. V. Andreeva, E. V. Skorb, *Langmuir* **2019**, *35*, 8543.
- [14] K. Lewis, A. M. Klibanov, *Trends Biotechnol.* **2005**, *23*, 343.
- [15] X. Zhu, X. J. Loh, *Biomater. Sci.* **2015**, *3*, 1505.
- [16] N. V. Ryzhkov, N. Brezhneva, E. V. Skorb, *Surf. Innovations* **2019**, *7*, 145.
- [17] B. Gottenbos, H. C. V. D. Mei, H. J. Busscher, *J. Biomed. Mater. Res.* **2000**, *50*, 208.
- [18] B. Gottenbos, *J. Antimicrob. Chemother.* **2001**, *48*, 7.
- [19] N. Kawabata, M. Nishiguchi, *Appl. Environ. Microbiol.* **1988**, *54*, 2532.
- [20] B. D. Wood, M. Quintard, S. Whitaker, *Biotechnol. Bioeng.* **2002**, *77*, 495.
- [21] C. D. L. Fuente-Núñez, F. Reffuveille, L. Fernández, R. E. Hancock, *Curr. Opin. Microbiol.* **2013**, *16*, 580.
- [22] H. Gu, S. Hou, C. Yongyat, S. D. Tore, D. Ren, *Langmuir* **2013**, *29*, 11145.
- [23] V. E. Johansen, L. Catón, R. Hamidjaja, E. Oosterink, B. D. Wilts, T. S. Rasmussen, M. M. Sherlock, C. J. Ingham, S. Vignolini, *Proc. Natl. Acad. Sci. USA* **2018**, *115*, 2652.
- [24] X. Jin, I. H. Riedel-Kruse, *Proc. Natl. Acad. Sci. USA* **2018**, *115*, 3698.

- [25] P. Q. Nguyen, Z. Botyanszki, P. K. R. Tay, N. S. Joshi, *Nat. Commun.* **2014**, *5*, 4945.
- [26] M. Florea, H. Hagemann, G. Santosa, J. Abbott, C. N. Micklem, X. Spencer-Milnes, L. D. A. Garcia, D. Paschou, C. Lazenbatt, D. Kong, H. Chughtai, K. Jensen, P. S. Freemont, R. Kitney, B. Reeve, T. Ellis, *Proc. Natl. Acad. Sci. USA* **2016**, *113*, E3431.
- [27] J. Huang, S. Liu, C. Zhang, X. Wang, J. Pu, F. Ba, S. Xue, H. Ye, T. Zhao, K. Li, Y. Wang, J. Zhang, L. Wang, C. Fan, T. K. Lu, C. Zhong, *Nat. Chem. Biol.* **2018**, *15*, 34.
- [28] L. Xu, Z. Zhu, S. A. Sukhishvili, *Langmuir* **2011**, *27*, 409.
- [29] Q. Yi, G. B. Sukhorukov, *Adv. Colloid Interface Sci.* **2014**, *207*, 280.
- [30] A. A. Antipov, G. B. Sukhorukov, H. Möhwald, *Langmuir* **2003**, *19*, 2444.
- [31] C. Déjugnat, G. B. Sukhorukov, *Langmuir* **2004**, *20*, 7265.
- [32] W. Tong, C. Gao, H. Möhwald, *Macromolecules* **2006**, *39*, 335.
- [33] S. A. Ulasevich, G. Brezesinski, H. Möhwald, P. Fratzl, F. H. Schacher, S. K. Poznyak, D. V. Andreeva, E. V. Skorb, *Angew. Chem., Int. Ed.* **2016**, *55*, 13001.
- [34] S. A. Ulasevich, N. Brezhneva, Y. Zhukova, H. Möhwald, P. Fratzl, F. H. Schacher, D. V. Sviridov, D. V. Andreeva, E. V. Skorb, *Macromol. Biosci.* **2016**, *16*, 1422.
- [35] J. Gensel, T. Borke, N. P. Pérez, A. Fery, D. V. Andreeva, E. Betthausen, A. H. E. Müller, H. Möhwald, E. V. Skorb, *Adv. Mater.* **2012**, *24*, 985.
- [36] D. O. Serra, A. M. Richter, R. Hengge, *J. Bacteriol.* **2013**, *195*, 5540.
- [37] W. Thongsomboon, D. O. Serra, A. Possling, C. Hadjineophytou, R. Hengge, L. Cegelski, *Science* **2018**, *359*, 334.
- [38] Y. Zhang, P. Batys, J. T. O'Neal, F. Li, M. Sammalkorpi, J. L. Lutkenhaus, *ACS Cent. Sci.* **2018**, *4*, 638.
- [39] T. Ikeda, H. Hirayama, H. Yamaguchi, S. Tazuke, M. Watanabe, *Antimicrob. Agents Chemother.* **1986**, *30*, 132.
- [40] D. J. Phillips, J. Harrison, S.-J. Richards, D. E. Mitchel, E. Tichauer, A. T. Hubbard, C. Guy, I. Hands-Portman, E. Fullam, M. I. Gibson, *Biomacromolecules* **2017**, *18*, 1592.
- [41] M. Wyrtywal, P. Koczurkiewicz, K. Wójcik, M. Michalik, B. Kozik, M. Żyłewski, M. Nowakowska, M. Kepczynski, *J. Biomed. Mater. Res., Part A* **2013**, *102*, 721.
- [42] G. Harkes, J. Dankert, J. Feijen, *J. Biomater. Sci., Polym. Ed.* **1992**, *3*, 403.
- [43] S. Trinschek, K. John, S. Lecuyer, U. Thiele, *Phys. Rev. Lett.* **2017**, *119*, 078003.
- [44] L. K. Koopal, *Adv. Colloid Interface Sci.* **2012**, *179*, 29.
- [45] M. Elzbiaciak, M. Kolasinska, P. Warszynski, *Colloids Surf., A* **2008**, *321*, 258.
- [46] A. V. Harpe, H. Petersen, Y. Li, T. Kissel, *J. Controlled Release* **2000**, *69*, 309.
- [47] K. A. Curtis, D. Miller, P. Millard, S. Basu, F. Horkay, P. L. Chandran, *PLoS One* **2016**, *11*, e0158147.
- [48] J. Suh, H. J. Paik, B. K. Hwang, *Bioorg. Chem.* **1994**, *22*, 318.
- [49] J. Goicoechea, F. J. Arregui, J. M. Corres, I. R. Matias, *J. Sens.* **2008**, *2008*, 142854.
- [50] S. W. Cranford, C. Ortiz, M. J. Buehler, *Soft Matter* **2010**, *6*, 4175.
- [51] A. S. Michaels, O. Morelos, *Ind. Eng. Chem.* **1955**, *47*, 1801.
- [52] J. Choi, M. F. Rubner, *Macromolecules* **2005**, *38*, 116.
- [53] J. Yan, C. Fei, S. Mao, A. Moreau, N. S. Wingreen, A. Košmrlj, H. A. Stone, B. L. Bassler, *eLife* **2019**, *8*, e43920.
- [54] J. Schindelin, I. Arganda-Carreras, E. Frise, V. Kaynig, M. Longair, T. Pietzsch, S. Preibisch, C. Rueden, S. Saalfeld, B. Schmid, J.-Y. Tinevez, D. J. White, V. Hartenstein, K. Eliceiri, P. Tomancak, A. Cardona, *Nat. Methods* **2012**, *9*, 676.